JOURNAL OF CATALYSIS 84, 38–44 (1983)

The Catalytic Oxidation of Propylene

X. An Investigation of the Kinetics and Mechanism over USb_3O_{10}

GEORGE W. KEULKS, ZUOLONG YU,[1] AND L. DAVID KRENZKE[2]

Department of Chemistry and Laboratory for Surface Studies, University of Wisconsin-Milwaukee, Milwaukee, Wisconsin 53201

Received October 25, 1982; revised June 13, 1983

The kinetics of propylene oxidation have been investigated over the temperature range 325 to 475°C. The reaction orders for both oxygen and propylene changed with temperature. At temperatures higher than 400°C, the reaction was first order in propylene pressure and zero order in oxygen pressure. At temperatures below 400°C, the reaction exhibited fractional order dependencies in both propylene and oxygen pressures. The apparent activation energy for acrolein formation changed from 17 kcal/mole at high temperatures to 30 kcal/mole at the lower temperatures. Oxygen-18 and deuterated propylene were used as tracers under steady-state reaction conditions. The tracer experiments indicated that acrolein is formed via a redox mechanism and that only a few layers of lattice oxygen participate in the reaction. The rate-limiting step is the abstraction of the α-hydrogen from propylene to form the allylic intermediate, but no isotope effect for the abstraction of the second hydrogen was observed. Carbon dioxide is formed through parallel and consecutive pathways.

INTRODUCTION

Various mixed oxides, such as Bi–Mo, Sn–Sb, and U–Sb oxides, have been shown to be efficient catalysts for the selective oxidation of propylene to acrolein. Although the Bi–Mo system has been studied extensively (*1–6*), the U–Sb system has received much less attention. Grasselli and Suresh (*7*) proposed that the oxidation of propylene over U–Sb oxide proceeds via a redox pathway, and the α-hydrogen abstraction from propylene is the rate-limiting step. Their results also suggested that a second hydrogen is abstracted before oxygen addition. Simons *et al.* (*8*) studied the oxidation of 1-butene over U–Sb oxide and their results indicated that only catalyst surface oxygen reacts in producing butadiene.

The purpose of this work was to investigate the kinetics and mechanism of propylene oxidation over pure USb_3O_{10} using oxygen-18 and 2,3,3,3-d_4-propylene as tracers in a flow reactor under steady-state conditions.

EXPERIMENTAL

1. Catalyst preparation. The uranium antimonate catalyst, USb_3O_{10}, was prepared according to Grasselli *et al.* (*7, 9*), by combining 75.6 g of Sb_2O_3, 28.5 g of $UO_2(NO_3)_2 \cdot 6H_2O$ and 337 ml 65% HNO_3 in a flask under reflux (110°C) for 3 h. The product was cooled and reduced to a pH of 8 by adding NH_4OH. The resultant slurry was filtered, dried at 120°C overnight, heated at 427°C for 16 h, and calcined at 927°C for 16 h. The excess antimony oxide was dissolved with HCl at 100°C. The catalyst then was washed with distilled water and dried at 120°C for 24 h. The final product was indicated to be pure USb_3O_{10} by XRD and ir analysis and had a BET surface area of 4.5 m^2/g.

2. Apparatus. The catalytic oxidation of propylene was carried out at atmospheric

[1] Chinese Academy of Sciences Visiting Scientist.

[2] Present address: Union Oil of California, Research Department, P.O. Box 76, Brea, California 92621.

0021-9517/83 $3.00

pressure in a fixed-bed, single-pass flow reactor described previously (*10*).

3. Procedure. The activity and selectivity of the catalyst were determined using 0.25 g of catalyst with a total gas flow of 60 (STP) cm^3/min, $C_3H_6 : O_2 : He = 3 : 3 : 4$.

In order to obtain accurate kinetic data, a small amount of catalyst charge, 0.25 g, was used. This served to reduce the possibility of developing temperature gradients in the catalyst bed. The conversion level was kept below 5% so that differential rate data could be obtained directly. In order to maintain a low conversion level with a fixed catalyst charge over a wide temperature range (325–475°C), the total flow rate was varied between 20 and 100 (STP) cm^3/min. The reaction orders for propylene and oxygen in both selective and nonselective oxidation were determined at seven different temperatures by the isolation method. The following partial pressures (in atmospheres) were used

He	O_2	C_3H_6
0.4	0.3	0.3
0.5	0.3	0.2
0.6	0.3	0.1
0.7	0.2	0.1
0.8	0.1	0.1

This data was used to calculate rate constants which were subsequently incorporated into Arrhenius plots to determine the apparent energies of activation for acrolein and carbon dioxide formation.

The oxygen-18 and 2,3,3,3-d_4-propylene tracer experiments were carried out following a similar procedure described in detail earlier (*11*).

RESULTS

1. Activity and Selectivity

Figure 1 shows that the activity of USb_3O_{10} increases gradually at temperatures lower than 400°C and then increases rapidly. The selectivity to acrolein, however, remains nearly constant over the entire temperature range.

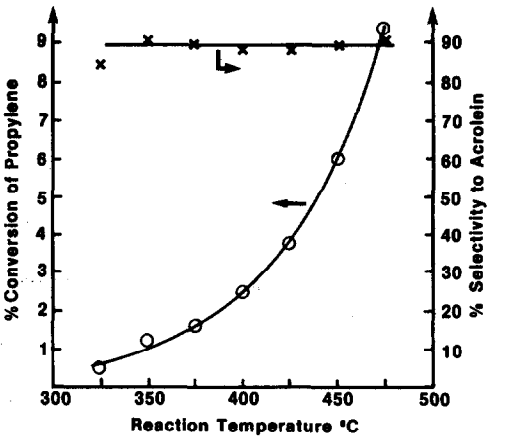

FIG. 1. Activity and selectivity of USb_3O_{10} for the catalytic oxidation of propylene as a function of temperature: ×, selectivity; ○, activity.

2. Kinetic Data

The data in Table 1 indicate that the reaction orders of both propylene and oxygen vary with temperature. The order in propylene for both acrolein and carbon dioxide formation decreases from first order at high temperature to a fractional order or zero order at low temperature. The order in oxygen for acrolein formation changes from zero at high temperature to a fractional order at low temperature. The formation of carbon dioxide exhibits a fractional order dependency on oxygen pressure, but the value increases as temperature decreases.

TABLE 1

Reaction Orders for Propylene Oxidation

Reaction temperature (°C)	C_3H_4O Formation		CO_2 Formation	
	C_3H_6	O_2	C_3H_6	O_2
475	1	0	1	0.2
450	1	0	0.9	0.3
425	1	0	0.6	0.5
411	0.6	0.2	0.3	0.7
375	0.4	0.3	0.1	0.7
351	0.4	0.3	0	0.8
325	0.2	0.4	0	0.8

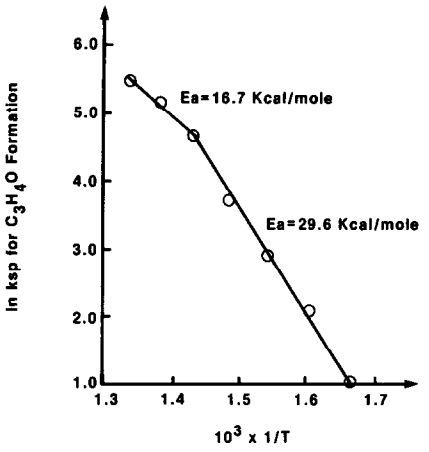

FIG. 2. Arrhenius plot for C_3H_4O formation. Formation using USb_3O_{10}.

The Arrhenius plots for acrolein and carbon dioxide formation over USb_3O_{10} are shown in Figs. 2 and 3.

The Arrhenius plots for acrolein and carbon dioxide formation both yield intersecting lines. The line representing the low temperature region yields a significantly higher activation energy than the line in the high temperature region.

3. *Oxygen-18 Data*

Using the oxygen-18 data and the following equation, the amount of the catalyst oxygen which participated in acrolein formation can be calculated

$$\frac{\%^{18}O \text{ in product}}{\%^{18}O \text{ in } O_2} = 1 - \exp(-Ft/V)$$

where $\%^{18}O$ in the product and $\%^{18}O$ in oxygen are determined by mass spectrometric analysis of the reactor effluent at time t. The total uptake of oxygen by the catalyst in microgram-atoms per min is designated as F. Under steady-state conditions, this value must be equivalent to the rate of removal of oxygen from the catalyst as oxygenated products and is obtained by GC analysis. The amount of catalyst oxygen which participates in the formation of a particular product, in μg atoms, can be determined from V, using a plot of $-\ln[1 - (\%^{18}O \text{ in product})/\%^{18}O \text{ in } O_2)]$ vs t.

Plots of $-\ln[1 - \%^{18}O \text{ in product}/\%^{18}O) \text{ in } O_2]$ vs t for experiments run at 450, 400, and 350°C are given in Fig. 4. The oxygen-18 data is calculated following the above procedure and is summarized in Table 2. The oxygen-18 data indicates that only 0.5 (at 350°C) and 1.7 (at 450°C) of the catalyst oxygen participates in the formation of acrolein. If one assumes that all the oxygen in the catalyst has an equal chance to participate in the reaction and that the oxygen packing density is 1×10^{15} atoms/cm^2, then

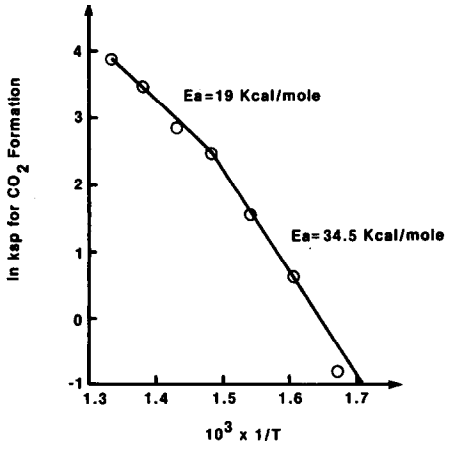

FIG. 3. Arrhenius plot for CO_2 formation. Formation using USb_3O_{10}.

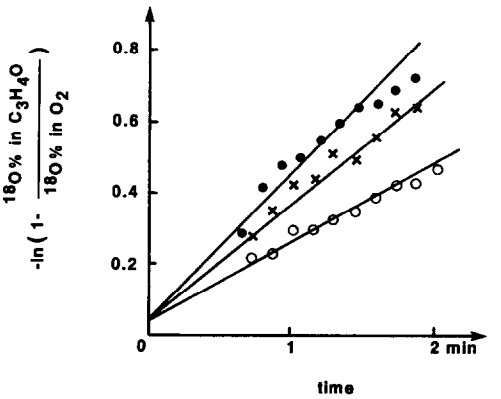

FIG. 4. ^{18}O Incorporation into C_3H_4O and CO_2 over USb_3O_{10} (○, 450°C; ×, 400°C; ●, 350°C).

TABLE 2

Summary of Oxygen-18 Data

Reaction temperature (°C)	F, Oxygen flow (μg-atoms/min)	Percentage of catalyst oxygen participating in the formation of C_3H_4O	Number of oxygen layers participating in the formation of C_3H_4O
450	46.4	1.7	3.0
400	19.1	0.9	1.7
350	8.1	0.5	1.0

only one layer (at 350°C) and three layers (at 450°C) of catalyst oxygen participate in selective oxidation of propylene. It should be noted that isotopic exchange reaction $^{32}O_2 + {}^{36}O_2 \rightleftarrows 2\,{}^{16}O{}^{18}O$ was not detected over USb_3O_{10} throughout the reaction temperature range.

4. *Oxidation of 2,3,3,3-d_4-Propylene*

The use of 2,3,3,3-d_4-propylene as an isotopic tracer is particularly useful in examining the rate limiting step for the conversion of propylene to acrolein. In addition, this reactant offers the advantage of probing the details of the sequence of carbon–hydrogen bond breaking and oxygen addition if one examines the deuterium distribution in the acrolein produced.

The experimentally observed values of the k_H/k_D ratios for the formation of acrolein and carbon dioxide are given in Table 3 and the deuterium distribution of the acrolein produced is given in Table 4. The approximate theoretical values for the kinetic isotope effect at the temperatures of the experiments were calculated from molecular data using the method described by Melander and Saunders (*12*).

TABLE 3

Oxidation of 2,3,3,-d_4-Propylene: K_H/K_D Ratios

	451°C		400°C		350°C	
Theoretical kinetic isotope effect	1.8		2.0		2.2	
Experimental data	C_3H_4O 1.5	CO_2 1.3	C_3H_4O 2.1	CO_2	C_3H_4O 2.5	CO_2 1.2

TABLE 4

Oxidation of 2,3,3,3-d_4-Propylene: Distribution of Deuterated Acroleins

Temp. (°C)	CD_2=CD—CHO (%)	CH_2=CD—CDO (%)
450	46	54
400	55	45
350	54	46
Theoretical for single isotope effect	51[a]	51
Theoretical for two isotope effects	64[a]	36

[a] Calculated at 450°C.

The salient facts from the isotopic tracer experiments are:

1. The experimentally observed k_H/k_D ratios are in good agreement with the calculated values.

2. The deuterium distribution in the acrolein produced indicates that each end of the allylic intermediate reacts with equal probability.

3. Intermolecular isotopic exchange is negligible. In addition, NMR analysis of the unreacted propylene indicated that double bond isomerization is also slow compared to reaction.

DISCUSSION

The results presented in Table 1 and Figs. 1 and 2 clearly indicate that the reaction exhibits different kinetics at low and high temperatures. When the reaction temperature is greater than 400°C, acrolein formation is first order in propylene pressure and zero order in oxygen pressure. At temperatures lower than 400°C, acrolein formation is fractional order in both propylene and oxygen pressures. The Arrhenius plots yield apparent activation energies of 16.7 and 29.6 kcal/mole in the high and low temperature regions, respectively.

The kinetic parameters observed for the USb_3O_{10} catalyst are quite similar to those observed for bismuth molybdate catalysts (*10, 13*). For the bismuth molybdate catalysts, the kinetics were interpretated in terms of a redox mechanism in which the rate limiting step changed from the abstraction of an allylic hydrogen at high temperatures to catalyst reoxidation at low temperatures. Thus, we believe the oxidation of propylene over USb_3O_{10} also occurs via a redox mechanism.

However, the kinetic parameters for the USb_3O_{10} catalyst differ from those observed with bismuth molybdate catalysts in two significant ways. First, a full primary isotope effect is observed for acrolein formation at both 350 and 450°C, but only a partial isotope effect is observed for carbon dioxide formation. Second, the apparent activation energy observed at the lower temperatures is 10–15 kcal/mole lower.

The observation of a full primary isotope effect for acrolein formation during the oxidation of 2,3,3,3-d_4-propylene (Table 3) strongly suggests that the rate limiting step is the abstraction of an allylic hydrogen. However, the lack of an isotope effect for the second hydrogen abstraction (Table 4) indicates that the sequence of C–H bond breaking and O-addition steps is different for the USb_3O_{10} catalyst compared to bismuth molybdate catalysts. Recently, Portefaix *et al.* (*14*) also reported the lack of an isotope effect for the second hydrogen abstraction for tin–antimony catalysts.

The lack of an isotope effect for the second hydrogen abstraction implies that over USb_3O_{10} and Sn–Sb catalysts the allylic intermediate adds oxygen *before* it loses a second hydrogen. Once the oxygen is added, subsequent steps involving breaking of a second C–H bond and acrolein desorption are fast at high temperature.

Our results are different from those reported by Grasselli and Suresh (*7*). However, it is important to note that Grasselli and Suresh (*7*) carried out their experiments in a pulse microreactor in the absence of gaseous oxygen, forcing the catalyst to function as the oxidant. We, on the other hand, have carried out our experiments in a flow microreactor in the presence of gaseous oxygen. We have observed recently, by using ir to study the rate of formation of surface intermediates, that the presence of gaseous oxygen greatly facilitates the abstraction of the second hydrogen (*15*). Thus, in the presence of gaseous oxygen, an isotope effect is detected for only the abstraction of the first oxygen. In the absence of gaseous oxygen, an isotope effect is observed for the abstraction of two hydrogens, in agreement with the earlier results reported by Grasselli and Suresh (*7*).

The lower apparent activation energy observed at the lower temperatures may be a result of two possibilities. First, it is possible that the lower activation energy indicates inhibition caused by strong adsorption of acrolein at lower temperatures. Support for this suggestion is offered by the results of Godin *et al.* (*16*), Vinogradova *et al.* (*17*), and Peacock *et al.* (*18*), who measured the activation energy for the desorption of acrolein over various mixed oxide catalysts. They reported values of 30–32 kcal/mole, which are in reasonable agreement with the value of 29.6 kcal/mole we observed. In addition, Batist *et al.* (*19*), and Linn and Sleight (*20*) reported a break in the activation energy near 400°C for the oxidation of 1-butene over bismuth molybdate and bismuth iron molybdate catalysts, which they attributed to the inhibition by butadiene at lower temperatures.

The second possibility is that catalyst reoxidation is rate limiting at low temperatures, as observed with bismuth molybdate catalysts. However, the 10–15 kcal/mole difference between bismuth molybdate and USb_3O_{10} may be due to the fact that only a few layers (Table 2) of lattice oxygen participate in the redox process with USb_3O_{10}. Our recent ir work (*15*) indicates that reoxidation of the surface layers by gaseous oxygen occurs with a lower apparent activa-

tion energy than for the bulk oxygen ions diffusing to the surface region. Therefore, since only a few layers of lattice oxygen participate in USb_3O_{10} compared to bismuth molybdate, the apparent activation energy for propylene oxidation at low temperatures will be less.

As indicated above, the oxygen-18 results presented in Table 2 indicate that only a very limited amount of the catalyst oxygen participates in the reaction. This result is consistent with the results of Grasselli *et al.* (*7*), who suggested that only a limited number of isolated, easily exchangeable oxygens are active. They calculated that the selective oxygen is limited to approximately 6% of the total available oxygen of the lattice.

The results presented in Table 1 indicate that the formation of carbon dioxide exhibits a fractional dependence on oxygen pressure throughout the entire temperature range. The data presented in Table 3 indicate that carbon dioxide formation yields only a partial kinetic isotope effect. These results can be interpreted by assuming carbon dioxide is produced via both consecutive and parallel pathways. In the consecutive pathway the carbon dioxide is produced by the consecutive oxidation of acrolein, in which a full isotope effect should be observed, while in the parallel pathway the carbon dioxide is produced by oxygen attack at the double bond of propylene. Since no C–H bond is involved in this process, no isotope effect should be observed. Thus according to this scheme, a partial kinetic isotope effect and a fractional order dependence on oxygen pressure are to be expected for the formation of carbon dioxide.

This interpretation is further substantiated by the change in selectivity observed with propylene compared to 2,3,3,3-d_4-propylene. In each case, the selectivity to acrolein was 3–5% less, for the oxidation of 2,3,3,3-d_4-propylene. Because the formation of acrolein from 2,3,3,3-d_4-propylene exhibits a full kinetic isotope effect over the temperature range studied, while the formation of carbon dioxide exhibits only a partial kinetic isotope effect, one expects that the selectivity to acrolein will be less from 2,3,3,3-d_4-propylene than from propylene.

CONCLUSIONS

The selective oxidation of propylene over USb_3O_{10} proceeds via a redox mechanism similar to that proposed for bismuth molybdate. The abstraction of an allylic hydrogen from propylene to form an allylic intermediate is the rate limiting step, but oxygen addition occurs before the abstraction of a second hydrogen. The selective oxygen is confined to a few percent of the total available. Carbon dioxide is formed via both consecutive and parallel pathways.

REFERENCES

1. Voge, H. H., and Adams, L. R., *Advan. Catal.* **17,** 151 (1967).
2. Margolis, L. Ya., *Catal. Rev.* **8,** 241 (1973).
3. Hucknall, D. J., "Selective Oxidation of Hydrocarbons," Chap. 3, p. 23. Academic Press, New York/London, 1974.
4. Keulks, G. W., Krenzke, L. D., and Notermann, T. M., *Advan. Catal.* **27,** 183 (1978).
5. Grasselli, R. K., and Burrington, J. D., *Advan. Catal.* **30,** 133 (1981).
6. Grasselli, R. K., Burrington, J. D., and Brazdil, J. F., *J. Chem. Soc. Faraday Disc.* **72,** 203 (1982).
7. Grasselli, R. K., and Suresh, D. D., *J. Catal.* **25,** 273 (1972).
8. Simons, Th. G. J., Houtman, P. N., and Schuit, G. C. A., *J. Catal.* **23,** 1 (1971).
9. Grasselli, R. K., and Callahan, J. L., *J. Catal.* **14,** 93 (1969).
10. Krenzke, L. D., and Keulks, G. W., *J. Catal.* **64,** 295 (1980).
11. Krenzke, L. D., and Keulks, G. W., *J. Catal.* **61,** 316 (1980).
12. Melander, L., and Saunders, W. K., Jr., "Reaction Rates of Isotopic Molecules," p. 130. Wiley, New York, 1980.
13. Monnier, J. R., and Keulks, G. W., *J. Catal.* **68,** 51 (1981).
14. Portefaix, J. L., Figuras, F., and Forissier, M., *J. Catal.* **63,** 307 (1980).

15. Yu, Z., and Keulks, G. W., in press.
16. Godin, G. W., McCain, C. C., and Porter, E. A., "Proceedings, 4th International Congress on Catalysis," Vol. 1, p. 271, 1971.
17. Vinogradova, O. M., Vytnov, G. Z., Luiksaar, I. V., and Al'tahuler, O. V., *Kinet. Katal.* **16,** 671 (1975).
18. Peacock, J. M., Parker, A. J., Ashmore, P. G., and Hockey, T. A., *J. Catal.* **15,** 398 (1969).
19. Batist, Ph, A., Der Kinderen, A. H. W. M., Leeuwenburg, Y., Metz, F. A. M. G., and Schuit, G. C. A., *J. Catal.* **12,** 45 (1968); **15,** 256.
20. Linn, W. J., and Sleight, A. W., *J. Catal.* **41,** 134 (1976).